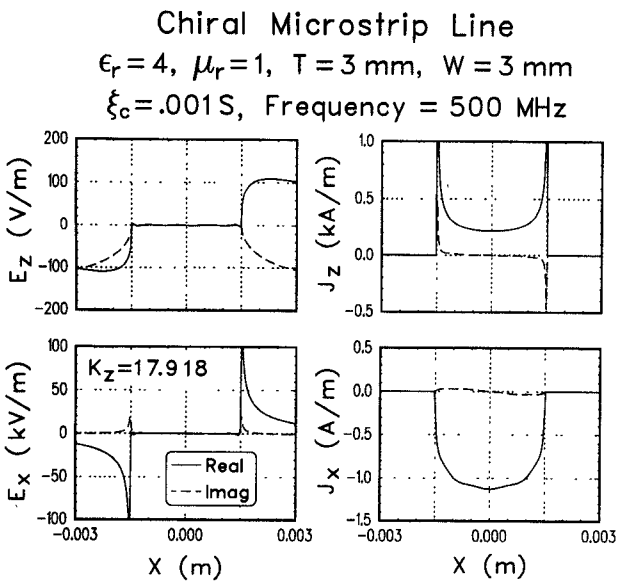

Fig. 2. Fields and currents at $y = T$ for a chiral microstrip solved using ten J_z modes and ten J_x modes.

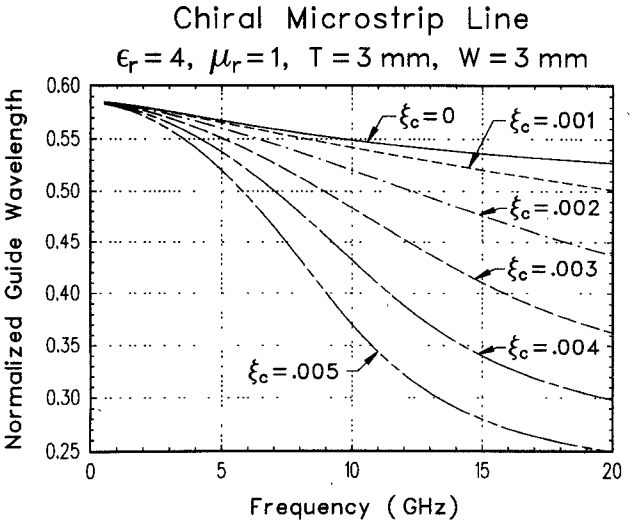

Fig. 3. Normalized guide wavelength (λ_g/λ_0) versus frequency for the fundamental mode of chiral and achiral microstrip lines, for a range of chiral parameters in Siemens.

$I_{z,0} = 1$, since the microstrip current can only be found to within a constant. In the figures the real part of the current and fields is shown as a solid line, and the imaginary part as a dashed line.

Fig. 2 shows the electric fields and currents at the interface $y = T$ for a MM solution using ten longitudinal and ten transverse basis functions. The left-hand graphs show that the fields satisfy the boundary condition of zero tangential electric field on the microstrip line. The corresponding currents are shown in the right-hand graphs. The even transverse current component, which occurs solely because of the chirality, is significantly larger than the odd transverse current component.

The dispersion curve shown in Fig. 3 shows the normalized guide wavelength (λ_g/λ_0) for the fundamental mode of a chiral microstrip line, for a range of chiral parameters. The case $\xi_c = 0$ corresponds to an achiral line. Fig. 3 shows that the propagation constant is not significantly affected unless the chiral parameter is a significant percentage of the maximum value set in [15] of $\xi_{c,\max} = \sqrt{\epsilon/\mu}$, which in this case is 0.0053 S.

References

[1] D. L. Jaggard, A. R. Mickelson, and C. H. Papas, "On electromagnetic waves in chiral media," *Appl. Phys.*, vol. 18, pp. 211–216, 1979.

[2] I. Tinoco, Jr. and M. P. Freeman, "The optical activity of oriented copper helices. I. Experimental," *J. Phys. Chem.*, vol. 61, pp. 1196–1200, Sept. 1957.

[3] E. J. Post, *Formal Structure of Electromagnetics*. Amsterdam: North-Holland, 1962.

[4] C. Eftimiu and L. W. Pearson, "Guided electromagnetic waves in chiral media," *Radio Science*, vol. 24, pp. 351–359, May/June 1989.

[5] P. Pelet and N. Engheta, "The theory of chirowaveguides," *IEEE Trans. Antennas Propagat.*, vol. AP-38, pp. 90–98, Jan. 1990.

[6] J. A. M. Svedin, "Propagation analysis of chirowaveguides using the finite-element method," *IEEE Trans. Microwave Theory Tech.*, vol. 38, pp. 1488–1496, Oct. 1990.

[7] M. S. Kluskens and E. H. Newman, "Scattering by a multilayer chiral cylinder," *IEEE Trans. Antennas Propagat.*, vol. AP-39, pp. 91–96, Jan. 1991.

[8] M. S. Kluskens, "Method of moments analysis of scattering by chiral media," Ph.D. dissertation, The Ohio State University, Columbus, June 1991.

[9] R. E. Collin, *Field Theory of Guided Waves*. New York: IEEE Press, 1991.

[10] T. Kitazawa and Y. Hayashi, "Propagation characteristics of striplines with multilayered anisotropic media," *IEEE Trans. Microwave Theory Tech.*, vol. 31, pp. 429–433, June 1983.

[11] F. Medina, M. Horno, and H. Baudrand, "Generalized spectral analysis of planar lines on layered media including uniaxial and biaxial dielectric substrates," *IEEE Trans. Microwave Theory Tech.*, vol. 37, pp. 504–511, Mar. 1989.

[12] M. Kobayashi and T. Iijima, "Frequency-dependent characteristics of current distributions on microstrip," *IEEE Trans. Microwave Theory Tech.*, vol. 37, pp. 799–801, Apr. 1989.

[13] Y. Yuan and D. P. Nyquist, "Full-wave perturbation theory based upon electric field integral equations for coupled microstrip transmission lines," *IEEE Trans. Microwave Theory Tech.*, vol. 38, pp. 1576–1584, Nov. 1990.

[14] I. S. Gradshteyn and I. M. Ryzhik, *Table of Integrals, Series, and Products*. Orlando, FL: Academic, 1980.

[15] N. Engheta and D. L. Jaggard, "Electromagnetic chirality and its applications," *IEEE Antennas and Propagation Society Newsletter*, vol. 30, pp. 6–12, Oct. 1988.

Time-Domain Scattering Parameters of an Exponential Transmission Line

Ching-Wen Hsue

Abstract—**The scattering parameters of an exponential line are studied in detail both in frequency and time domains. By taking the causality condition into consideration, we cast the time domain scattering parameters in a rapid-convergence power series. Each term of the power series represents a signal component generated by the exponential line when the signal travels a round trip.**

Manuscript received April 30, 1991; revised June 17, 1991.

The author is with AT&T Bell Laboratories, P.O. Box 900, Princeton, NJ 08540.

IEEE Log Number 9102815.

I. Introduction

Time-domain transmission line analysis has been a subject of interest in recent microwave studies [1]–[12]. Due to its potential applications in high-speed circuit designs, most of the investigations [1]–[8] focused on the formulation of electromagnetic waves along the transmission media in terms of time and space variables. Some [9]–[12] examined the dispersion effect of lossy or dispersive transmission media on the pulse signal degradation. For the analysis of linear circuits, we use frequency-domain scattering parameters to evaluate the circuit performance. The time-domain responses of such circuits are obtained by taking the inverse Laplace transforms of the corresponding frequency-domain functions. However, when transmission lines are terminated with nonlinear loads, the above technique is no longer an adequate approach [2], [3]. A more appropriate approach is to characterize the transmission line by a set of time-domain scattering parameters, so that the interaction between the transmission line and nonlinear loads can be expressed by the corresponding time-domain convolution integral. To investigate the time-domain responses involving signal lines and nonlinear loads, it is therefore pertinent to study time-domain scattering parameters of the transmission lines.

Frequency- and time-domain scattering parameters of a uniform signal line had been studied extensively in the past [1]–[12]. To the author's knowledge, no literature had treated the time-domain scattering parameters of an exponential line analytically. The work reported here is partly motivated by our desire to study the interaction of nonuniform lines with nonlinear loads. Here we limit our attention to the time-domain characteristics of an exponential line. We first present the frequency-domain scattering parameters of a lossless, exponential transmission line. The time-domain scattering parameters are then obtained by taking the inverse Laplace's transform of their corresponding functions in the frequency domain.

II. Scattering Parameters in Frequency Domain

We show in Fig. 1 that a nonuniform transmission line can be described as a set of scattering parameters which relate two reflected waves and two incident waves:

$$b_1(s) = \tilde{S}_{11}(s)a_1(s) + \tilde{S}_{12}(s)a_2(s), \tag{1}$$

$$b_2(s) = \tilde{S}_{21}(s)a_1(s) + \tilde{S}_{22}(s)a_2(s), \tag{2}$$

where $a_1(s)$, $b_1(s)$, $a_2(s)$, $b_2(s)$ are the incident and reflected waves for ports 1 and 2 respectively, $\tilde{S}_{ij}(s)$ $(i,j=1,2)$ are the scattering parameters, and s represents the frequency. Specifically, $\tilde{S}_{11}, \tilde{S}_{22}$ are treated as scattering reflection coefficients, while $\tilde{S}_{12}, \tilde{S}_{21}$ are regarded as the scattering transmission coefficients. The nonuniform line extends over a distance l and is terminated with two uniform reference lines at both ends. For convenience, we choose $Z_{\text{ref},1}$ and $Z_{\text{ref},2}$ as the source (left) and load (right) end reference impedances, which are equal to the characteristic impedances of the exponential line at the left and right sides, respectively.

To evaluate the scattering parameters of the exponential line, we consider a lossless, nonuniform line having a characteristic impedance as follows,

$$Z(x) = Z_S e^{\gamma x}, \tag{3}$$

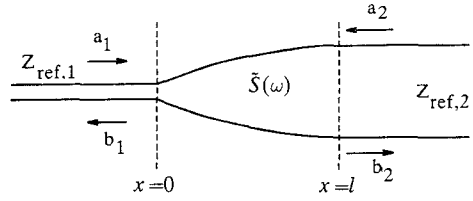

Fig. 1. Scattering parameters representation of a nonuniform transmission line.

with

$$\gamma = \frac{\ln(Z_L/Z_S)}{l}, \tag{4}$$

where Z_S and Z_L are the characteristic impedances at the left (source) and right (load) of the exponential line, respectively. The exponential line extends from $x=0$ to $x=l$. The frequency domain voltage and current along an exponential line can be expressed as [13]:

$$V(x) = A_1 e^{\gamma x/2} e^{-j\kappa x} + A_2 e^{\gamma x/2} e^{j\kappa x} \tag{5}$$

and

$$I(x) = A_1 \frac{\kappa + j\gamma/2}{\omega L_o} e^{-\gamma x/2} e^{-j\kappa x} - A_2 \frac{\kappa - j\gamma/2}{\omega L_o} e^{-\gamma x/2} e^{j\kappa x}, \tag{6}$$

respectively, where ω is the angular frequency and

$$\kappa = \left(\omega^2 LC - \frac{\gamma^2}{4}\right)^{1/2}, \tag{7a}$$

$$L = L_o e^{\gamma x}, \tag{7b}$$

$$C = C_o e^{-\gamma x}. \tag{7c}$$

Note that L_o and C_o represent the inductance and capacitance per unit length at the input end of the nonuniform line, i.e., $Z_S = (L_o/C_o)^{1/2}$. The first term of right hand side in (5) denotes a forward $(+x)$ traveling wave while the second term designates a backward $(-x)$ traveling wave. A_1 and A_2 in (5) and (6) are determined by the boundary conditions. At the load end, we have

$$\left.\frac{V(x)}{I(x)}\right|_{x=l} = Z_L. \tag{8}$$

Upon substitution of (5), (6), into (8), we obtain the relation between A_1 and A_2. At the input end, we get the input impedance Z_{in}

$$\left.\frac{V(x)}{I(x)}\right|_{x=0} = Z_{\text{in}}. \tag{9}$$

The incident wave $V_{\text{inc.}}$ is related to A_1 and A_2 in the form of

$$V_{\text{inc.}} = \frac{A_1 + A_2}{1+\rho}, \tag{10}$$

where ρ is the reflection coefficient at the input end, which is given by

$$\rho = \frac{Z_{\text{in}} - Z_S}{Z_{\text{in}} + Z_S}. \tag{11}$$

The transmission coefficient at the load end is defined as the ratio of the transmitted wave to the incident wave. If we divide

(5) by (10), after some algebraic manipulations, we get the transmission coefficient ξ

$$\xi = \frac{V_{x=l}}{V_{\text{inc.}}} = \left(\frac{Z_L}{Z_S}\right)^{1/2} \frac{2\left(1-\gamma^2/4k_o^2\right)^{1/2} e^{-j(k_o^2-\gamma^2/4)1/2 l}}{\left[1+\left(1-\gamma^2/4k_o^2\right)^{1/2}\right] + e^{-j2(k_o^2-\gamma^2/4)1/2 l}\left[-1+\left(1-\gamma^2/4k_o^2\right)^{1/2}\right]}, \tag{12}$$

where the propagation constant k_o is

$$k_o = \omega(L_o C_o)^{1/2}. \tag{13}$$

In the above evaluation for the transmission coefficient ξ, we assume the exponential line is terminated with a matching transmission line of characteristic impedance Z_L. For such a situation, the reflected wave vanishes, i.e., $a_2(s) = 0$ in (2). Equation (2) reveals that the scattering transmission parameter $\tilde{S}_{21}$ is the ratio of $b_2(s)$ to $a_1(s)$, which are equal to $V_{x=l}$ and $V_{\text{inc.}}$, respectively. This, in turn, indicates that ξ is equivalent to the scattering parameter $\tilde{S}_{21}(s)$. If we substitute $s = j\omega$, $v = (L_o C_o)^{-1/2}$ into (12) and remove the normalized impedance factor $(Z_L/Z_S)^{1/2}$, we get the scattering transmission parameter:

$$\tilde{S}_{21}(s) = \frac{2\left(s^2+\gamma^2 v^2/4\right)^{1/2} e^{-(s^2+\gamma^2 v^2/4)^{1/2} l/v}}{\left[s+\left(s^2+\gamma^2 v^2/4\right)^{1/2}\right] + \left[-s+\left(s^2+\gamma^2 v^2/4\right)^{1/2}\right] e^{-2(s^2+\gamma^2 v^2/4)^{1/2} l/v}}. \tag{14}$$

The reciprocity principle indicates that

$$\tilde{S}_{12}(s) = \tilde{S}_{21}(s). \tag{15}$$

Substituting (5)–(9) into (11), we get the expression for the reflection coefficient ρ at the input end, which is equal to the scattering reflection coefficient $\tilde{S}_{11}(s)$:

$$\tilde{S}_{11}(s) = \rho = \frac{\gamma v}{2} \frac{1 - e^{-2(s^2+\gamma^2 v^2/4)^{1/2} l/v}}{\left[s+\left(s^2+\gamma^2 v^2/4\right)^{1/2}\right] + \left[-s+\left(s^2+\gamma^2 v^2/4\right)^{1/2}\right] e^{-2(s^2+\gamma^2 v^2/4)^{1/2} l/v}}. \tag{16}$$

Equation (16) indicates that $\tilde{S}_{11}(s)$ is an odd function of γ. If we invert the impedance ratio of Z_L to Z_S, as can be inferred from (4), γ changes the sign. Therefore, the scattering parameter $\tilde{S}_{22}(s)$ at the load end is

$$\tilde{S}_{22}(s) = -\tilde{S}_{11}(s). \tag{17}$$

It is pertinent to point out that the above scattering transmission coefficients $\tilde{S}_{ij}(s)$ $(i \neq j)$ are valid for the power evaluation. The scattering transmission coefficients should accompany the appropriate normalized impedance factors when they are used for the transient voltage calculation.

III. Time Domain Scattering Parameters

The time domain scattering parameters $S_{ij}(t)$ are the inverse Laplace's transforms of the frequency domain scattering parameters. This gives

$$S_{ij}(t) = L^{-1}\left[\tilde{S}_{ij}(s)\right], \qquad (i,j=1,2) \tag{18}$$

where L^{-1} represents the inverse Laplace transforms. To perform the inverse Laplace transforms, we first rearrange the scattering parameter $\tilde{S}_{21}(s)$ and expand it into a power series,

$$\tilde{S}_{21}(s) = \frac{2\left(s^2+\gamma^2 v^2/4\right)^{1/2}}{s+\left(s^2+\gamma^2 v^2/4\right)^{1/2}} e^{-(s^2+\gamma^2 v^2/4)^{1/2} l/v} \cdot \frac{1}{1+\dfrac{-s+\left(s^2+\gamma^2 v^2/4\right)^{1/2}}{s+\left(s^2+\gamma^2 v^2/4\right)^{1/2}} e^{-2(s^2+\gamma^2 v^2/4)^{1/2} l/v}} \tag{19a}$$

$$\approx \frac{2\left(s^2+\gamma^2 v^2/4\right)^{1/2}}{s+\left(s^2+\gamma^2 v^2/4\right)^{1/2}} e^{-(s^2+\gamma^2 v^2/4)^{1/2} l/v} - \frac{\gamma^2 v^2/2\left(s^2+\gamma^2 v^2/4\right)}{\left[\left(s^2+\gamma^2 v^2/4\right)^{1/2}\right]\left[s+\left(s^2+\gamma^2 v^2/4\right)^{1/2}\right]^3} \cdot e^{-3(s^2+\gamma^2 v^2/4)^{1/2} l/v} + \cdots. \tag{19b}$$

Although $\tilde{S}_{21}(s)$ consists of an infinite number of terms, causality condition makes it physically sound to consider the first few terms of the power series expansion [1]. We may expand the same function in terms of a finite sum with a remainder instead of as an infinite series. As will be clear later, the high-order

terms represent the signal contribution which occurs in lagged time intervals. For many practical applications, we use scattering parameters to analyze the transient behaviors of transmission line systems. The transient responses will eventually reach the steady state value which is determined by the source and load resistances but not by the characteristic impedances of the nonuniform transmission line [6]. The high-order terms have no or less contribution to the first arriving wave, transition ripple and the steady state value. Therefore, when the time domain scattering parameters are used to evaluate the transient responses of transmission systems, the high-order terms can be neglected. For the present consideration, we focus on the first two terms of $\tilde{S}_{21}(s)$. Of course, if it is necessary, we can take more terms into consideration. The inverse Laplace transforms of $\tilde{S}_{21}(s)$ can be obtained with the aid of tabulated transforms [14]. We introduce

$$L^{-1}\{\alpha^{\beta} r^{-1} R^{-\beta} e^{-br}\} = \begin{cases} 0 & 0 < t < b \\ (t-b)^{1/2\beta}(t+b)^{-1/2\beta} J_{\beta}(\alpha y) & t > b \end{cases} \tag{20}$$

where

$$r = (s^2 + \alpha^2)^{1/2} \tag{21a}$$

$$R = s + r \tag{21b}$$

$$y = (t^2 - b^2)^{1/2}, \tag{21c}$$

and $J_{\beta}(\alpha y)$ represents the Bessel function of the first kind, β order. Furthermore, the transform of differentiation gives [14]:

$$L\left\{\frac{d^n}{dt^n} f(t)\right\} = s^n F(s) - s^{n-1} f(0+) - \cdots - \frac{d^{n-1}}{dt^{n-1}} f(0+), \tag{22}$$

where L designates the Laplace transform and $F(s)$ is the transform of $f(t)$. In order to simplify the expression, we define the propagation delay over the nonuniform line as

$$\frac{l}{v} = 1. \tag{23}$$

Substituting (20)–(23) into (19b), we get the time domain scattering parameter $S_{21}(t)$,

$$S_{21}(t) \approx 2\frac{d^2}{dt^2}[f_1] + \frac{\gamma^2 v^2}{2}[f_1] - \frac{\gamma^2 v^2}{2}\frac{d^2}{dt^2}[f_2] - \frac{\gamma^4 v^4}{8}[f_2], \tag{24}$$

where

$$f_1 = \frac{2}{\gamma v}(t-1)^{1/2}(t+1)^{-1/2} J_1\left(\frac{\gamma v}{2}[t^2-1]^{1/2}\right) u_{-1}(t-1), \tag{25}$$

$$f_2 = \frac{8}{\gamma^3 v^3}(t-3)^{3/2}(t+3)^{-3/2} J_3\left(\frac{\gamma u}{2}[t^2-9]^{1/2}\right) u_{-1}(t-3), \tag{26}$$

and $u_{-1}(t-1)$ is the unit step function commencing at $t=1$. Note that f_1 has a contribution to $S_{21}(t)$ for $t>1$, while f_2 yields contribution to $S_{21}(t)$ for $t>3$. $S_{21}(t)$ has been normalized with respect to the propagation delay time across the nonuniform line. The first two terms in (24) are the inverse transforms of the first term in (19b), whereas the remainders in (24) represent the inverse transforms of the second term in (19b). Fig. 2 shows the time domain scattering transmission coefficient $S_{21}(t)$ for two impedance ratios $Z_L/Z_S = 4, 9$. $\delta(t-1)$ represents the impulse delta function commencing at $t=1$ and should be included for both cases. The steady state value of $S_{21}(t)$ is zero, which can be obtained from (14). Note that Fig. 2 designates the impulse responses at the load end when the input is excited by an impulse delta function.

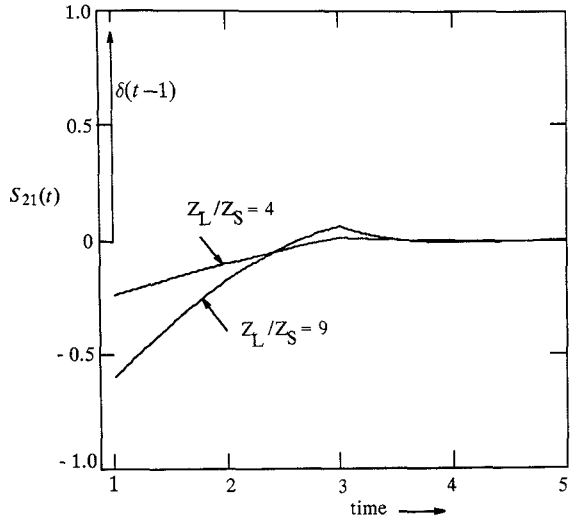

Fig. 2. Time-domain scattering transmission coefficient $S_{21}(t)$ of an exponential line.

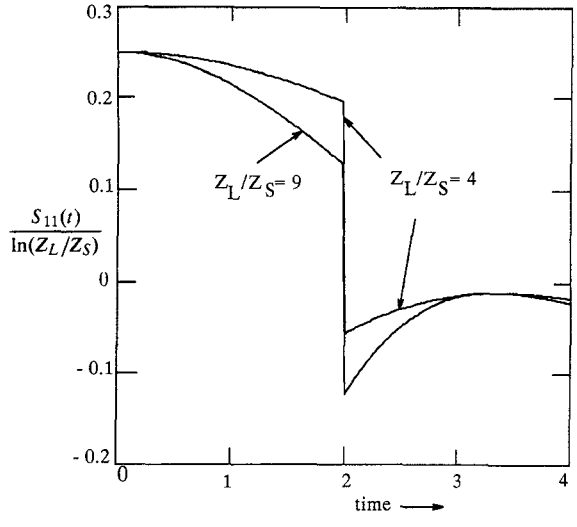

Fig. 3. Time-domain scattering reflection coefficient $S_{11}(t)$ of an exponential line.

By expanding $\tilde{S}_{11}(s)$ into a power series, we obtain

$$\tilde{S}_{11}(s) \approx \frac{\gamma v/2}{s + (s^2 + \gamma^2 v^2/4)^{1/2}} - \frac{\gamma v (s^2 + \gamma^2 v^2/4)^{1/2}}{\left[s + (s^2 + \gamma^2 v^2/4)^{1/2}\right]^2} \cdot e^{-2(s^2+\gamma^2 v^2/4)^{1/2} l/v}. \tag{27}$$

We introduce [14]:

$$L^{-1}\{R^{-n}\} = n\alpha^{-n} t^{-1} J_n(\alpha t), \tag{28}$$

where R is defined in (21b). The inverse transform of $\tilde{S}_{11}(s)$ is

$$S_{11}(t) \approx [f_3] - \gamma v \frac{d^2}{dt^2}[f_4] - \frac{\gamma^3 v^3}{4}[f_4], \tag{29}$$

where

$$f_3 = t^{-1} J_1\left(\frac{\gamma v}{2} t\right) u_{-1}(t), \tag{30}$$

$$f_4 = \frac{4}{\gamma^2 v^2}(t-2)(t+2)^{-1} J_2\left(\frac{\gamma v}{2}[t^2-4]^{1/2}\right) u_{-1}(t-2). \tag{31}$$

When $t < 2$, f_3 represents the reflected wave at the input end before the first reflection returns. Fig. 3 shows the time domain scattering reflection parameter $S_{11}(t)$ for two impedance ratios $Z_L/Z_S = 4, 9$. Note that $S_{11}(t)$ is normalized with respect to a factor $\ln(Z_L/Z_S)$. The drop of $S_{11}(t)$ at $t = 2$ is 0.25 for both impedance ratios. Equations (24) and (29) reveal that $S_{21}(t)$ is an even function of γ while $S_{11}(t)$ is an odd function of γ.

IV. Conclusion

Exact solutions are found for both the frequency domain and time domain scattering parameters of an exponential transmission line. The time domain scattering parameters of an exponential line lay the foundation for the studies of interaction between nonuniform lines and linear/nonlinear loads, and pulse waveform alteration in the time domain.

References

[1] C. T. Tai, "Transients on lossless terminated transmission lines," *IEEE Trans. Antennas Propagat.*, vol. AP-26, pp. 556–561, July 1978.

[2] J. E. Schutt-Aine and R. Mittra, "Scattering parameter transient analysis of transmission lines loaded with nonlinear terminations," *IEEE Trans. Microwave Theory Tech.*, vol. 36, pp. 529–536, Mar. 1988.

[3] A. R. Djordjevic, T. K. Sarkar, and R. F. Harrington, "Analysis of transmission lines with arbitrary nonlinear terminal networks," *IEEE Trans. Microwave Theory Tech.*, vol. MTT-21, pp. 660–666, June 1986.

[4] H. Mohammadian and C. T. Tai, "A general method of transient analysis for a lossless transmission line and its analytical solution to time-varying resistive terminations," *IEEE Trans. Antennas Propagat.*, vol. AP-32, pp. 309–312, Mar. 1984.

[5] Q. Gu and J. A. Kong, "Transient analysis of single and coupled lines with capacitively-loaded junctions," *IEEE Trans. Microwave Theory Tech.*, vol. MTT-34, pp. 952–964, Sept. 1986.

[6] C.-W. Hsue, "Elimination of ring signals for a lossless, multiple-section transmission line," *IEEE Trans. Microwave Theory Tech.*, vol. 37, pp. 1178–1183, Aug. 1989.

[7] I. L. Hill and D. Mathews, "Transient analysis of systems with exponential lines," *IEEE Trans. Microwave Theory Tech.*, vol. MTT-25, pp. 777–783, Sept. 1977.

[8] E. R. Schatz and E. M. Williams, "Pulse transients in exponential transmission lines," *Proc. I.R.E.*, vol. 27, pp. 65–71, Oct. 1950.

[9] R. J. Veghte and C. A. Balanis, "Dispersion of transient signals in microstrip transmission lines," *IEEE Trans. Microwave Theory Tech.*, vol. MTT-34, pp. 1427–1436, Dec. 1986.

[10] C. D. Hechtman and C.-W. Hsue, "Transient analysis of a step wave propagating in a lossy dielectric," *J. Appl. Phys.*, vol. 65, pp. 3335–3339, May 1989.

[11] ____, "Time domain scattering parameters for a lossy dielectric," *J. Appl. Phys.*, vol. 67, pp. 2199–2209, Mar. 1990.

[12] G.-C. Liang, Y.-W. Liu, and K. K. Mei, "Full-wave analysis of coplanar waveguide and slotline using the time-domain finite-difference method," *IEEE Trans. Microwave Theory Tech.*, vol. 37, pp. 1949–1957, Dec. 1989.

[13] W. C. Johnson, *Transmission Lines and Networks*. New York: McGraw-Hill, 1950.

[14] A. Erdelyi *et al.*, *Table of Integral Transforms*. New York: McGraw-Hill, 1954.

Analysis of 3-D Microwave Resonators using Covariant-Projection Elements

J. P. Webb and Ruth Miniowitz

***Abstract*—Three-dimensional microwave resonators of arbitrary shape can be analyzed with the finite element method using covariant-projection elements, curvilinear bricks which impose only tangential field continuity. The method produces no spurious modes, and works well even when sharp metal edges are present. The matrices involved, though large, are sparse; an appropriate sparse eigenvalue algorithm allows the method to run in modest amounts of memory. Results are presented for a number of test cases, including a rectangular microstrip resonator.**

I. Introduction

ELECTROMAGNETIC resonance is important in the operation of many microwave devices, and its prediction has been the subject of a large number of papers. For structures of arbitrary shape, numerical methods are necessary. The finite element method has long been used for finding the modes of uniform waveguides [1], and has been proposed as a technique for 3-D cavity resonance [2], [3]. However, several obstacles have impeded the application of 3-D elements. The problem of spurious modes has, rightly, received the most attention, and the last few years have seen the publication of a variety of solutions, both in 2-D and in 3-D [2]–[7]. However, a second difficulty which arises commonly in microwave devices is that of sharp conducting edges and corners. To find resonances, it is usually necessary to solve for the electric or magnetic field directly, and these fields are, in general, infinite at sharp edges. The continuous, piecewise-polynomial variations provided by conventional finite elements do not adequately represent such singularities, and lead to poor results [8], [9].

One answer is to add to the polynomials special trial functions capable of modeling the singularity [8]. A different, and in many ways more elegant, solution is provided by the work of Crowley *et al.* [10], [11] on new finite elements capable of avoiding spurious modes. These are called covariant-projection elements. Covariant-projection elements only enforce the tangential continuity of the vector field, leaving the normal component at interfaces free to adopt its natural value. This reduced continuity appears to allow a better modeling of singularities. A version of the elements was tried in 2-D for the analysis of uniform waveguides with sharp edges, with excellent results [12]. Crowley *et al.* demonstrated the validity of the brick element for several 3-D cavity problems, but none had sharp metal edges. It is the purpose of this paper to show that covariant-projection elements, combined with a suitable sparse-matrix solution of the algebraic problem, is an effective method for 3-D cavity resonance, even when singularities are present.

Manuscript received November 5, 1990; revised June 27, 1991. This work was supported by the Natural Sciences and Engineering Research Council of Canada.

J. P. Webb is with the Computational Analysis and Design Laboratory, Department of Electrical Engineering, McGill University, 3480 University Street, Montreal, PQ H3A 2A7, Canada.

R. Miniowitz was with the Computational Analysis and Design Laboratory, Department of Electrical Engineering, McGill University, Montreal, PQ, Canada. She is currently with the Electromagnetics Department, RAFAEL, P.O. Box 2250, Haifa 31021, Israel.

IEEE Log Number 9102822.